End effects in falling-ball viscometry

By R. I. TANNER

Department of Mechanical Engineering, University of Sydney

(Received 3 September 1962 and in revised form 14 January 1963)

A calculation taking into account the interaction of tube wall and ends with a falling sphere is presented, with a view to assessing the change in drag on the sphere due to the end proximity in practical viscometry. It is shown that when the sphere is more than one fall tube radius from the closed end, the extra drag resulting is less than $4{\cdot}5 \times 10^{-3}$ of the Faxèn drag, and is therefore usually negligible.

For smaller end-sphere distances the end-effect drag increases rapidly, reaching about 1·5 of the Faxèn drag when the sphere centre is 0·25 tube radius from the end. The drag curve lies substantially below that given by Ladenburg (1907). Satisfactory agreement with experiment is found. It is concluded that with the commonly used types of fall tubes, end effects due to a closed end and an open surface will not be detectable.

1. Introduction

In many cases high viscosities (> 10 poise) may be most conveniently measured by the falling-ball technique. As the fluid becomes more viscous, so it becomes a more convenient method compared with capillary tube viscometry, especially in laboratories where highly viscous liquids are only occasionally dealt with. In practical measurements, various corrections for departures from Stokes's law for an unbounded fluid have to be applied. Of these, the Faxèn (1923) correction for the extra drag due to the proximity of the fall-tube walls is well known to be accurate, and is recommended for use by standard handbooks (British Standards Institution 1957) on viscometry. It may be recalled that the total drag D of a sphere (radius a) falling axially at speed U in fluid of viscosity η, and enclosed in an infinitely long tube of radius R_0, is given by

$$D = D_s[1 + 2{\cdot}1048a/R_0 + O(a^3/R_0^3)], \tag{1}$$

where $D_s \equiv 6\pi\eta aU$ is the Stokes drag and the other terms in (1) represent the Faxèn correction in Stokes's flow (zero Reynolds number); inertia is ignored in the present paper. However, the Faxèn correction applies to an infinitely long tube, and it is clear that the presence of a fixed closed end (or an open end) will also affect the drag on the sphere. Merrington (1949) states that the correction for finite tube length is 'probably negligible'. This is in accordance with the account of Barr (1931), who suggests that the end correction tends to vanish when the distance of the ball from the end is comparable to the fall tube radius, and at variance with Ladenburg's (1907) calculation. Ladenburg (1907), using a calcula-

tion of Lorentz (1907), valid for a sphere approaching an infinite plane surface, suggested that the ends increased the average resistance over the central $\frac{5}{12}$ of the tube in the ratio $(1 + 3{\cdot}3a/L) : 1$, where L is the tube length. Since this amounts to an increase of several per cent for a typical practical arrangement, and no such increase is noted, it is known to be much too large. For the configuration to which it applies, the Lorentz formula is known to give reasonable agreement with experiment (Altrichter & Lüstig 1937), but it does *not* apply to end effects in falling-sphere viscometry. A calculation which obtains a result similar to those of Lorentz (1907) and Ladenburg (1907) has recently been published by Maude (1961). Again, no account is taken of the interaction between tube walls and ends, although Brenner (1961) has pointed out its importance. Hence no realistic calculation of the magnitude of end effects in practical viscometry is known to the author. An attempt to fill this gap is presented here.

The method adopted is the classical 'method of reflexions' developed by Lorentz (1907). It is necessary to evaluate the velocities in the Faxèn solution in the plane of the cylinder ends. Then a solution of the creeping flow equations with zero velocity over the cylindrical wall and velocities which are the negative of the 'unsatisfied' velocities on the ends must be found. Addition of this velocity field will result in zero boundary velocities over the entire cylinder. The resulting drag increment from this additional reflexion may be estimated using the Faxèn (1923)–Pérès (1929) method. Using this, it is only necessary to estimate the reflected velocity $\mathbf{v}^{(3)}$ at the sphere centre; the drag increment is then $6\pi\eta a v_z^{(3)}$. This is correct as far as terms in a/R_0 or a/Z (where Z is the end-sphere distance) whichever is larger; higher-order terms are not considered. The paper concludes with a discussion of end effects in practical situations.

2. General approach and boundary conditions

The method of reflexions successively approximates to the true solution of the sphere in the tube problem by satisfying boundary conditions at the sphere and the tube wall alternately. Each successive reflexion cancels out the unsatisfied velocity component on one solid surface and thereby reduces the velocity there to zero, introducing a reflected error at the other solid surface. Thus a gradual approach to the true velocity field $\mathbf{v}$ is obtained, giving $\mathbf{v} = \mathbf{v}^{(0)} + \mathbf{v}^{(1)} + \mathbf{v}^{(2)} + \ldots$ as the sum of the reflected fields. If R and Z are cylindrical polar co-ordinates, and $\mathbf{i}_Z$, $\mathbf{i}_R$ are corresponding unit vectors, then the field $\mathbf{v}^{(0)}$ is simply $-U\mathbf{i}_Z$. On the assumption that the fluid boundaries are sufficiently distant from the sphere centre, so that terms of order a^3/r^3 may be neglected in comparison with a/r (r is the radial distance from the sphere centre) on the boundaries, the field $\mathbf{v}^{(1)}$ may be taken as a 'Stokeslet' flow:

$$\mathbf{v}^{(1)} \equiv \tfrac{3}{4}U\{2(a/R)\,\mathbf{i}_Z - a\nabla(Z/R)\}, \tag{2}$$

The field $\mathbf{v}^{(2)}$ is given in integral form by Brenner & Happel (1958) for an infinitely long tube. If solid ends are now considered, then a further field $\mathbf{v}^{(3)}$ is needed to cancel unsatisfied velocities on the ends; $\mathbf{v}^{(3)}$ must not re-introduce velocities on the tube walls.

The velocity vector $\mathbf{v}^{(2)}$ for a centrally falling sphere is given by the following expression (Brenner & Happel 1958):

$$\frac{\mathbf{v}^{(2)}}{U} = -\frac{3a}{2\pi}\mathbf{i}_R \int_0^\infty [\psi_0(\lambda) I_0'(\lambda R) + \pi_0(\lambda)\lambda R I_0''(\lambda R)] \sin \lambda Z \, d\lambda$$

$$-\frac{3a}{2\pi}\mathbf{i}_Z \int_0^\infty [\psi_0(\lambda) I_0(\lambda R) + \pi_0(\lambda)\lambda R I_0'(\lambda R) + \pi_0(\lambda) I_0(\lambda R)] \cos \lambda Z \, d\lambda, \quad (3)$$

where

$$\pi_0(\lambda) \equiv \frac{K_0(\lambda R_0)}{I_0(\lambda R_0)} + \frac{I_0'(\lambda R_0)}{I_0(\lambda R_0)} [\lambda R_0 I_0^2(\lambda R_0) - 2 I_0(\lambda R_0) I_0'(\lambda R_0) - \lambda R_0 I_0'^2(\lambda R_0)]^{-1}, \quad (4)$$

$$\psi_0(\lambda) \equiv -[1 + \lambda R_0 I_0'(\lambda R_0)/I_0(\lambda R_0)] \pi_0(\lambda)$$

$$+ [\lambda R_0 K_0'(\lambda R_0) + 2 K_0(\lambda R_0)] [I_0(\lambda R_0)]^{-1}. \quad (5)$$

Here I_0, K_0 are the modified Bessel functions of order zero.

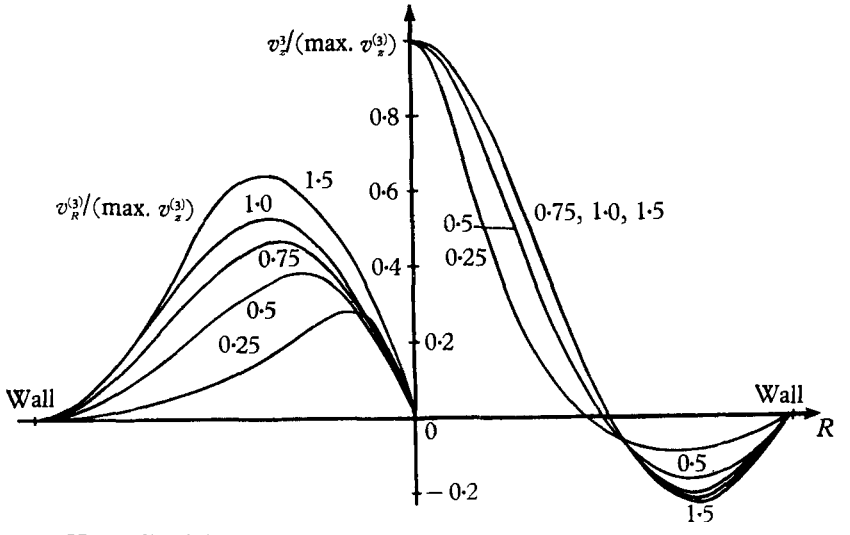

FIGURE 1. Normalized 'unsatisfied' velocity profiles for various Z/R_0. Here max. $v_Z^{(3)}$ (see table 1) is the value of $v_Z^{(3)}$ on the tube axis.

Boundary conditions given in the integral form (3) scarcely encourage one to look for a wholly analytical solution, so expression (3) was evaluated at ten equi-spaced points on the tube radius for various sphere-end distances Z/R_0. A programme was written for the Sydney University SILLIAC computer which evaluated $\mathbf{v}^{(3)} = \mathbf{v}^{(2)} + \mathbf{v}^{(1)}$ at sphere-end distances of 0·25, 0·5, 0·75, 1·0, 1·5 and 2·0 tube radii. The Bessel functions I_0, I_1 and K_0 were generated to 6–7 figure accuracy (mainly limited by K_0) and K_1 was found from the well-known relation

$$I_0(x) K_1(x) + I_1(x) K_0(x) = x^{-1}. \quad (6)$$

The integrations were performed using Filon's (1928) modification of Simpson's rule. Step lengths and upper limits of integration were chosen to give a final accuracy of the order of 1 part in 10^4 for $\mathbf{v}^{(3)}/U$. Results are shown in figure 1, where all velocities are referred to the velocity $\mathbf{v}_Z^{(3)}$ on the tube axis. The curve for

$Z/R_0 = 2$ is omitted as the integration accuracy for this case is of the same order as the velocity magnitudes.

Table 1 gives the magnitudes of $v_Z^{(3)}R_0/Ua$ on the tube axis for various Z/R_0. Extension to higher values of Z/R_0 is clearly unnecessary. As a comparison, the corresponding velocity for the unbounded Stokeslet flow (equation (2)) is also given.

Z/R_0	$\frac{v_Z^{(3)}R_0}{Ua}$ (at $R = 0$)	$\frac{v_Z^{(3)}R_0}{Ua}$ (Stokeslet flow $R = 0$)
0·25	3·9644	6·0
0·5	1·1464	3·0
0·75	0·3854	2·0
1·0	0·1271	1·5
1·5	0·0105	1·0
2·0	0·0004	0·75

TABLE 1. Maximum axial velocity at various Z/R_0.

It is seen that the effect of the tube walls is to reduce by very large factors the residual velocities remaining to be 'reflected' by the ends except for small Z/R_0; thus we may anticipate that the Ladenburg (1907) result will generally be much too large.

As a partial check on the numerical results, the velocity on the axis was evaluated analytically. The Z-component of equation (3) with $R = 0$ may be rewritten in the form

$$-\frac{2\pi}{3}\frac{v_Z^{(2)}}{U}\frac{R_0}{a}\bigg|_{R=0} = 2\int_0^\infty \frac{K_0(\lambda)}{I_0(\lambda)}\cos\frac{Z\lambda}{R_0}\,d\lambda + \int_0^\infty \frac{2I_1(\lambda)-\lambda I_0(\lambda)}{I_0(\lambda)\,\Delta(\lambda)}\cos\frac{Z\lambda}{R_0}\,d\lambda$$
$$\equiv \mathscr{I}_1 + \mathscr{I}_2, \quad \text{say,} \tag{7}$$

where $\Delta(\lambda) \equiv \lambda I_0^2 - 2I_0 I_1 - \lambda I_1^2$.

Consider the first integral $\mathscr{I}_1$ in (7). This may be written, using the definition of K_0 (McLachlan 1955), as

$$\mathscr{I}_1 = 2\int_0^\infty -(\lambda + \ln\tfrac{1}{2}\lambda)\cos\frac{Z\lambda}{R_0}\,d\lambda$$
$$+ 2\int_0^\infty \sum_{m=1}^{\infty}\left[\frac{(\frac{1}{2}\lambda)^{2m}\{1+\frac{1}{2}+\frac{1}{3}+\ldots+1/m\}}{I_0(\lambda)\,(m!)^2}\right]\left(\cos\frac{Z\lambda}{R_0}\right)d\lambda. \tag{8}$$

The first part of $\mathscr{I}_1$ is simply $\pi R_0/|Z|$ ($|Z| > 0$) (Lighthill 1958). The second part is analytic in the complex plane except at the zeros of $I_0(\lambda)$. It may be shown that each term of (8) vanishes on a large semicircular contour in the upper half-plane and on using the residue calculus one can express $\mathscr{I}_1$ in the form

$$\mathscr{I}_1 = \pi\left[\frac{R_0}{Z} - \pi\sum_{\alpha_n}\frac{Y_0(\alpha_n)\exp(-Z\alpha_n/R_0)}{J_1(\alpha_n)}\right] \quad (z > 0), \tag{9}$$

where the α_n are the roots of $J_0(\alpha) = 0$; (J_0, Y_0, and J_1 are the Bessel functions of the first and second kinds, order zero, and the first kind, order one, respectively).

The integral $\mathscr{I}_2$ may also be evaluated using the residue calculus, the result being

$$\mathscr{I}_2 = 2\pi \sum_{\alpha_n} \frac{\exp(-Z\alpha_n/R_0)}{\alpha_n J_1^2(\alpha_n)} + \frac{\pi}{2} \mathrm{Re}\left[\sum_{\beta_n} \frac{i\beta_n \exp(iZ\beta_n/R_0)}{I_0^2(\beta_n)}\right], \tag{10}$$

where β_n are the roots of $\Delta = 0$ (equation (7)).

Summing the various expressions (9), (10) and the Z-component of (2) finally gives

$$\left.\frac{v_Z^{(3)}}{U}\frac{R_0}{a}\right|_{R=0} = -\frac{3}{4}\sum_{\beta_n} \frac{i\beta_n \exp(-i\beta_n Z/R_0)}{J_0^2(i\beta_n)}. \tag{11}$$

The roots (β_n) of Δ included within the integration contour in the upper half plane are of the form $\pm a_n + ib_n$; hence the $i\beta_n$ are complex conjugates of the form $-b_n \pm ia_n$, and equation (11) is purely real. The first four $i\beta_n$ values are given in Appendix 1, table 5; each term contains an exponential decay factor $e^{-b_n Z/R_0}$, so for large values of Z/R_0 only a few terms of the series are needed. Evaluation is tedious with existing tables, and it was found that only values for $Z/R_0 > 1$ could easily be calculated accurately. The values obtained, 0·0102 (0·0105 computed) and 0·0003 (0·0004 computed) for $Z/R_0 = 1{\cdot}5$ and 2·0 respectively, confirm that the numerical calculations of velocities are subject to errors in the region of 10^{-4}.

To estimate the change in drag, it is only necessary to find the value of $v_Z^{(3)}$ induced at the sphere centre (Pérès 1929) by a flow satisfying the creeping flow equations and with velocities $-(\mathbf{v}^{(1)} + \mathbf{v}^{(2)})$ over the ends and zero on the cylindrical surface.

It is convenient to define all lengths in terms of the tube radius R_0, writing $\rho = R/R_0$, $z = Z/R_0$. By using the Stokes stream function (Lamb 1945) ψ to define

$$v_R = \frac{1}{\rho}\frac{\partial \psi}{\partial z}, \quad v_Z = -\frac{1}{\rho}\frac{\partial \psi}{\partial \rho},$$

the continuity equation is automatically satisfied. The creeping flow equations are satisfied if ψ is a solution of

$$E^2\psi \equiv [\partial^2/\partial\rho^2 - (1/\rho)\,\partial/\partial\rho + \partial^2/\partial z^2]^2\,\psi = 0. \tag{12}$$

It was decided to find a semi-analytical solution to the problem using a variational method. Purely numerical methods such as relaxation (Allen 1954) or 'squaring' (Thom & Apelt 1961) tend to converge slowly for fourth-order equations; on the other hand, the Ritz and Galerkin variational processes often produce exceedingly good results with little work for fourth-order equations (Krylov & Kantorovitch 1958). A further factor influencing the choice in the present instance was computer availability; nearly all the numerical work was done by standard routines on SILLIAC without the need to write the large programme necessary for a purely numerical method. In the Galerkin procedure a set of functions which satisfies all the boundary conditions of the problem, but not the partial differential equation, is specified. For example, assume that

$$\psi = \sum_{i=1}^{r} \chi_i. \tag{13}$$

In the present case each χ_i is assumed to be of the form $f_i(z)\, g_i(\rho)$. Here $g_i(\rho)$ is a polynomial arranged to satisfy some of the boundary conditions on ψ and $f_i(z)$ is as yet undetermined. To find the $f_i(z)$ each χ_i is made orthogonal to $E^2\psi$ over the region of interest. Here we put

$$\iint E^2\psi\chi_i \frac{d\rho}{\rho} dz = 0 \quad (i = 1, 2, \ldots, r), \tag{14}$$

the integral being taken over the limits $\rho = 0$ to 1, z over the whole tube length. The results of the single integration with respect to ρ leaves a set of r ordinary differential equations for finding the f_i. Solution of these with appropriate boundary conditions produces an approximation to the solution of the original partial differential equation. The number of terms taken (r) is determined by the accuracy required.

The factor $1/\rho$ which has been inserted in (14) ensures that the Galerkin 'solution' coincides with the Ritz (1908) variational 'solution'. The Ritz method applied to the present case minimizes the total rate of energy dissipation over the entire fluid volume (subject to the constraints imposed by the choice of the boundary velocities). Helmholtz's theorem (Lamb 1945) shows that the true solution of the creeping flow equation (12) with given boundary conditions is that giving the least rate of dissipation. Thus when a very large number of terms are taken, the Galerkin and Ritz methods converge towards the true solution. [It may readily be shown by the aid of Green's theorem (see Krylov & Kantorovitch 1958) that the Galerkin 'solution' and that obtained from the same choice χ_i by minimizing the rate of energy dissipation are indeed the same]. In practice, with partial differential equations of the type discussed here, it is often found that only a few terms are needed to provide a good approximation to the solution. Further discussion of the Ritz and Galerkin methods is to be found in the book by Krylov & Kantorovitch (1958).

Assume that the cylinder is semi-infinite in the positive z-direction and that the closed end contains the origin. A set of functions χ_i satisfying the velocity boundary conditions on the cylindrical surface is

$$\chi_i = (1-\rho^2)^2\rho^{2i} f_i(z), \quad \psi = \sum_{i=1}^{r} \chi_i. \tag{15}$$

Working out the orthogonality integrals (14) gives the following set of equations for the f_i:

$$\sum_{i=1}^{r} (a_{ij}\, d^4/dz^4 + b_{ij}\, d^2/dz^2 + c_{ij}) f_i = 0, \quad (j = 1, \ldots, r), \tag{16}$$

where
$$a_{nm} \equiv 12(m+n-1)!/(m+n+4)!,$$
$$b_{nm} \equiv -16\{6mn-(m+n)\, mn-1\}\,(m+n-2)!/(m+n+3)!,$$
$$c_{nm} \equiv 192mn(mn-1)\,(m+n-3)!/(m+n+2)!.$$

Assuming a solution of the form $e^{\lambda z}$ and solving the equation arising from the determinant of the linear equations gives a set of approximate eigenvalues (λ),

which compares closely with the true eigenvalues (Appendix). The approximate eigenvalues obtained for $r = 1, 2, 3$ and 4 are:

$$r = 1\text{: } \pm 4{\cdot}354 \pm 1{\cdot}719i;$$

$$r = 2\text{: } \pm 4{\cdot}455 \pm 1{\cdot}467i;\ \pm 7{\cdot}630 \pm 2{\cdot}951i;$$

$$r = 3\text{: } \pm 4{\cdot}466 \pm 1{\cdot}467i;\ \pm 7{\cdot}587 \pm 1{\cdot}842i;\ \pm 11{\cdot}422 \pm 4{\cdot}812i;$$

$$r = 4\text{: } \pm 4{\cdot}46630 \pm 1{\cdot}46747i;\ \pm 7{\cdot}68536 \pm 1{\cdot}72545i;$$

$$\pm 10{\cdot}69484 \pm 2{\cdot}50578i;\ \pm 15{\cdot}91534 \pm 7{\cdot}15643i.$$

Discarding the solutions with positive real parts (so that the velocities vanish as z becomes very large) shows that the f_i must have the form

$$f_i(z) = \sum_{k=1}^{r} \exp(-\mu_k z)\{A_{ik} \sin \nu_k z + B_{ik} \cos \nu_k z\}, \tag{17}$$

where μ_k, ν_k are the magnitudes of the real and imaginary parts, respectively, of the kth eigenvalue.

Z/R_0	No. of terms, r	Mean percentage error in: Axial velocity	Mean percentage error in: Radial velocity
0·25	4	3·4	1·8
0·5	4	0·72	0·41
0·75	4	0·37	0·080
1·0	4	0·045	0·015
1·5	3	0·20	0·05

TABLE 2. Accuracy of least-squares fit of boundary conditions.

Least-squares fitting using the velocity distributions calculated in § 2 provide values of $f_i(0)$ and $f_i'(0)$. Hence 21 relations between the A_{ik} and B_{ik} are obtained from equations (17). A further set of relations exist which ensure that the equations (17) are solutions of the equations (16), so that a total of 21^2 linear equations is obtained from which the A_{ik} and B_{ik} may be found. Solving for the A_{ik} and B_{ik} gives the solution for the $f_i(z)$ and hence the value of $v_Z^{(3)}$ at the sphere centre. For $Z/R_0 \geqslant 0{\cdot}5$ this process rapidly produced a solution which fitted the boundary values of velocity closely. Taking $\Sigma\,|\text{error}|/\Sigma\,|v^{(3)}|$ as a measure of error, this measure reduces by a factor of at least 5 as r increases by one for $Z/R_0 \geqslant 0{\cdot}5$. For $Z/R_0 = 0{\cdot}25$, convergence was slower, and 0·5 appears to be about the lowest value of Z/R_0 which can be effectively tackled by the present method. The percentage accuracy of fit, judged by the value of

$$10\Sigma\,|\text{error}|/\text{max.}\,|v_Z^{(3)}|$$

(i.e. fitted over 10 points, taking the average value) is given in table 2. The decrease of accuracy for small Z/R_0 is to be noted.

3. Results and discussion

The drag increment as a fraction of the Stokes drag is simply $v_Z^{(3)}/U$ evaluated at the ball centre.† The sequence of values obtained by taking 1, 2, 3 and 4 terms in the Galerkin method are given in table 3, together with an extrapolated value and an estimate of the accuracy.

	Number of terms, r				$\frac{v_Z^{(3)}}{U_Z^{(3)}}\frac{R_0}{a}$	Estimated
Z/R_0	1	2	3	4	(final estimate)	accuracy (%)
0·25	2·247	2·334	2·382	2·460	~3·0	~ ±10
0·5	0·417	0·431	0·444	0·436	0·442	± ½
0·75	0·0622	0·0704	0·0720	0·0725	0·0728	± ½
1·0	0·01180	0·00907	0·00933	0·00938	0·0094	±1
1·5	$2{\cdot}66\times10^{-5}$	$7{\cdot}08\times10^{-5}$	$7{\cdot}45\times10^{-5}$	$7{\cdot}51\times10^{-5}$	$7{\cdot}6\times10^{-5}$	±1

TABLE 3. Drag increments $(v_Z^{(3)}/U)\,(R_0/a)$ due to closed end.

The extrapolated values were found using Salzer's (1954) method for monotonic sequences. Rapid convergence was obtained except for $Z/R_0 = 0{\cdot}25$. The present method is not very effective for this case, and it would probably be more economical to restart the calculation from the Lorentz (1907) solution if such low values of Z/R_0 were of interest.

Figure 2 shows the results for the complete drag curve. The Ladenburg drag curve shown is the sum of the Faxèn drag and the Lorentz (1907) end-effect correction. The latter amounts to a drag increase of $\frac{9}{8}D_s(a/Z)$. The present results lie above the Faxèn and Lorentz curves taken separately, but well below the sum of the two. In fact, the sphere drag appears to be little greater than the larger of the Faxèn or Lorentz drags.

A short experimental investigation using a 40 mm diameter fall tube, $\frac{1}{16}$ in. diameter steel balls and a 1000 poise (approx.) silicone fluid was made. The balls were timed over successive 5 mm intervals corresponding to $Z/R_0 = \ldots, 1, \frac{3}{4}, \frac{1}{2}, \frac{1}{4}$, several tests being made. The estimated timing accuracy was ~ 1 %. The ratios of average speed over an interval to average speed over an interval a long way from the end are compared in table 4. Satisfactory agreement with theory is noted.

For end-sphere distances greater than $1{\cdot}5R_0$ no explicit values of the drag increment have been found. However, inspection of the solution (18) and the magnitude of the unsatisfied boundary velocities (11) suggests that the end-effect correction $v_Z^{(3)}/U$ may be represented for large values of Z/R_0 by

$$(a/R_0)\,C(Z/R_0)\exp(-8{\cdot}933Z/R_0),$$

where $C(Z/R_0)$ is a slowly varying function, whose magnitude is in the range 30–80 in the cases examined. Also, for tubes longer than about two diameters, it may be readily demonstrated numerically that the two ends will have a

† The referee has kindly supplied a proof showing that the addition of a rigid wall must increase the drag.

negligible effect on one another, and the distant end may be ignored. However, for shorter tubes reflexions from both ends must be considered.

Returning to the viscometry problem, it is clear that Barr's (1931) remark (that end effects are negligible when the sphere is about one tube radius from the end) which is presumably based on observation, is completely justified for closed ends.

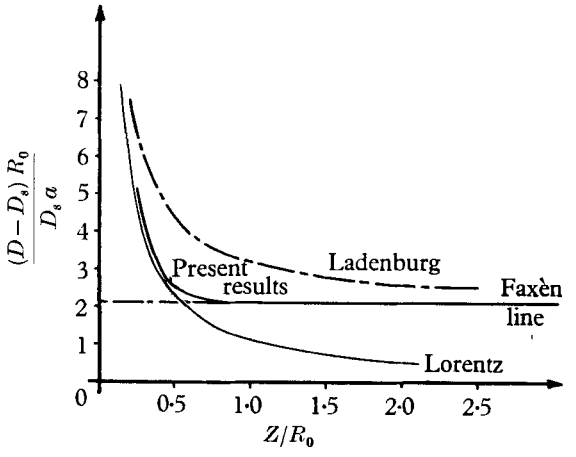

FIGURE 2. Drag curves.

Average Z/R_0 of interval	Speed ratio (experiment)	Speed ratio (predicted)
$\frac{3}{8}$	0·95	0·96
$\frac{5}{8}$	0·99	0·99
$\frac{7}{8}$	1·00	1·00
$1\frac{1}{8}$	1·00	1·00

TABLE 4. Comparison of theory and experiment.

An open end would require the vanishing of stresses at the free surface (Brenner 1961), and would involve repeating the calculation with different boundary conditions. However, the eigenvalues remain the same as in the closed-end case, and hence the same rapid attenuation of the end effect must occur. Hence it is clear that the practice of ignoring end effects in viscometry is generally correct; in particular, no sensible error will result from this cause when using the fall tubes described in B.S.S. **188**, 1957.

Appendix. Comparison of exact and variational eigenvalues

Elementary solutions of the creeping flow equation (12) finite at the origin are

$$\psi = \{A_\lambda \lambda^2 \rho^2 J_0(\lambda\rho) + B_\lambda \lambda \rho J_1(\lambda\rho)\} e^{\lambda Z}, \tag{18}$$

where A_λ, B_λ are constants, and λ a parameter.

To satisfy the boundary conditions of zero velocity on the cylinder $\rho = 1$ one has $\dfrac{\partial\psi}{\partial\rho} = \dfrac{\partial\psi}{\partial z} = 0$ on $\rho = 1$, giving the equations

$$A_\lambda \lambda^2 J_0(\lambda) + B_\lambda \lambda J_1(\lambda) = 0, \tag{19}$$

$$A_\lambda\{2\lambda J_0 - \lambda^2 J_1\} + B_\lambda\{\lambda J_0\} = 0. \tag{20}$$

Hence the equation for the eigenvalues λ becomes

$$\lambda J_0^2 - 2J_0 J_1 + \lambda J_1^2 = 0. \tag{21}$$

The magnitudes of the first four eigenvalues (after the obvious one $\lambda = 0$) are shown in table 5. They were found by Newton's method, working with complex arithmetic on SILLIAC. Initial guesses were supplied from a preliminary plot of the expression (21).

The comparison with the first two Galerkin eigenvalues is excellent. Accuracy is limited to 5–6 figures.

	Real part		Imaginary part	
No. of eigenvalue	Exact equation	4-term Galerkin	Exact equation	4-term Galerkin
1	4·46631	4·46630	1·46745	1·46747
2	7·69410	7·68536	1·72697	1·72545
3	10·8746	10·6948	1·89494	2·50578
4	14·0389	15·9153	2·02006	7·15643

TABLE 5. Comparison of eigenvalues.

REFERENCES

ALLEN, D. N. DE G. 1954 *Relaxation Methods in Engineering and Science.* New York: McGraw-Hill.

ALTRICHTER, F. & LÜSTIG, A. 1937 *Phys. Z.* **38**, 786.

BARR, G. 1931 *A Monograph of Viscometry*, p. 184. Oxford University Press.

BRENNER, H. 1961 *Chem. Eng. Sci.* **16**, 242.

BRENNER, H. & HAPPEL, J. 1958 *J. Fluid Mech.* **4**, 195.

BRITISH STANDARDS INSTITUTION 1957 *Determination of Absolute Viscosity in c.g.s. Units, B.S.S.* **188**, 1957 (London).

FAXÈN, H. 1923 *Ark. Mat. Astr. Fys.* **17**, 1.

FILON, L. N. G. 1928 *Proc. Roy. Soc. Edinb.* **49**, 38.

KRYLOV, V. I. & KANTOROVITCH, LV. (translated by BENSTER, C. D.) 1958 *Approximate Methods of Higher Analysis*, ch. 4. Groningen: Noordhoff.

LADENBURG, R. 1907 *Ann. Phys., Lpz.* (4), **23**, 447.

LAMB, H. 1945 *Hydrodynamics*, p. 125. New York: Dover.

LIGHTHILL, M. J. 1958 *An Introduction to Fourier Analysis and Generalised Functions.* Cambridge University Press.

LORENTZ, H. A. 1907 *Abh. Theor. Phys.* **1**, 23. Berlin: B. G. Teubner.

MCLACHLAN, N. M. 1955 *Bessel Functions for Engineers.* Oxford University Press.

MAUDE, A. D. 1961 *Brit. J. Appl. Phys.* **12**, 293.

MERRINGTON, A. C. 1949 *Viscometry*, p. 48. London: Arnold.

PÉRÈS, J. 1929 *C.R. Acad. Sci., Paris*, **188**, 310.

RITZ, W. 1908 *J. reine angew. Math.* **135**, 1.

SALZER, H. E. 1954 *J. Math. Phys.* **33**, 356.

THOM, A. & APELT, C. J. 1961 *Field Computations in Engineering and Physics.* New York: Van Nostrand.